Minimum Impulse Three-Body Trajectories

LOUIS A. D'AMARIO* AND THEODORE N. EDELBAUM†
The Charles Stark Draper Laboratory, Inc., Cambridge, Mass.

A rapid and accurate method of calculating optimal impulsive transfers in the restricted problem of three bodies has been developed. The technique combines a multiconic method of trajectory integration with primer vector theory and an accelerated gradient method of trajectory optimization. A unique feature is that the state transition matrix and the primer vector are found analytically without additional integrations or differentiations. The method has been applied to the determination of optimal two- and three-impulse transfers between the L_2 libration point and circular orbits about both the Earth and the moon.

Introduction

ALMOST all of the work done on space trajectory optimization to date has been concerned with two-body trajectory optimization. The great majority of the more than three hundred references in the Gobetz and Doll survey of impulsive trajectories[1] are concerned with inverse square fields. In fact the organization of their survey is based entirely on the two-body problem. For the two-body problem, both the trajectory and its state transition matrix can be calculated analytically. However, it is generally necessary to use numerical methods to optimize two-body transfers. Effective techniques have been developed by combining primer vector theory with accelerated gradient techniques.[2-4] For the three-body problem, both the trajectory and its state transition matrix must be calculated numerically Analytic approximations such as the patched conic method,[5] and the method of matched asymptotic expansions[6-8] have inherent accuracy limitations and break down completely for some missions of interest, such as trajectories to the collinear libration points[9-11] of a three-body problem. Even numerical integration of the state and the transition matrix for the three-body problem presents difficulties because of the singularities at the center of each body. Also, since a large number of trajectories and state transition matrices must be calculated in the process of converging to an optimal trajectory, the computer time with this approach can easily become prohibitive.

Recently a new approach to the integration of the N-body problem has been tried. This approach was conceived independently by several investigators[12-14] and actually constitutes a class of closely related methods. One of the most fruitful points of view is to regard them as large step numerical integration formulas. Instead of being based on polynomials, as are most conventional numerical integration formulas, these methods are based on two-body conics. The oldest of these methods is the "N-body reference orbit" of Stumpff and Weiss.[12] The N-body reference orbit is an analytic approximation to the true three-body trajectory. In their approach, two-body conics of each body with respect to each of the other bodies are used. All conics are propagated forward in time from the initial state. The method also uses linear, field-free trajectories which go backwards in time. Weiss later showed[17] that the state transition matrix may be obtained analytically. As the state transition matrix is normally found by integrating the six-by-six matrix of variational equations or by a numerical differentiation which requires the calculation of seven trajectories, this represents a very substantial savings in time. The other two methods[13,14] were developed subsequently to calculate trajectories from the Earth to the moon. Wilson[13] developed his method for the three-body problem and derived two alternate ways to calculate the trajectory depending upon whether the spacecraft is moving from the Earth to the moon or vice-versa. The two-body conics used in this method are propagated from different starting points and are connected by linear field-free trajectories. The multiconic method of Byrnes and Hooper,[14] which was conceived independently, is in effect an extension of Wilson's method to account for the effects of Earth oblateness and a fourth body, the sun. However, both these effects are included in a linear manner.

The present report is the first attempt known to the authors to apply this type of approach to three-body trajectory optimization. The method used combines Wilson's multiconic method of trajectory propagation, primer vector theory, and a recently developed accelerated gradient functional minimization algorithm.[16] The result is a rapid and efficient method of calculating optimal three-impulse, three-body trajectories. The method readily extends to N bodies and M impulses.

Trajectory Propagation

Position and Velocity

The model for the Earth-moon system used in this study is that of the restricted problem of three bodies. The third body, the spacecraft, is assumed to have negligible mass so that it is affected by but does not affect the motion of the other two bodies. A multiconic approximation as formulated by Wilson[13] will provide a solution to this problem useful as a state vector propagation algorithm which is much faster than numerical integration of the equations of motion yet of comparable accuracy. The multiconic approximation is a numerical integration technique which uses very large step sizes and yields very good accuracy. The multiconic approximation spans the range between the extremely fast but relatively inaccurate patched conic methods and the slow but very accurate numerical integration techniques.

The geometry of the three-body problem is illustrated in Fig. 1. Assuming that the only forces acting are the central force fields of the Earth and the moon and that the mass of the spacecraft is negligible, the accelerations are

$$\ddot{\bar{R}} = -(A\bar{R}/R^3)-(a\bar{r}/r^3)-(a\bar{\rho}/\rho^3) \quad (1)$$

$$\ddot{\bar{r}} = -(a\bar{r}/r^3)-(A\bar{R}/R^3)+(A\bar{\rho}/\rho^3) \quad (2)$$

$$\ddot{\bar{\rho}} = -\alpha\bar{\rho}/\rho^3 \quad (3)$$

where A and a are the gravitational parameters of the Earth and moon, respectively, and $\alpha = A+a$. The positions and velocities of the three bodies at any time t_j are related by

Presented as Paper 73-145 at the AIAA 11th Aerospace Sciences Meeting, Washington, D.C., January 10–12, 1973; submitted January 19, 1973; revision received August 16, 1973. This report was prepared under DSR Project 56-40024, sponsored by the NASA Goddard Space Flight Center, through Grant NGR 22-009-207, Supplement No. 5.

Index category: Lunar and Interplanetary Trajectories.

* Research Staff. Member AIAA.

† Research Staff. Associate Fellow AIAA.

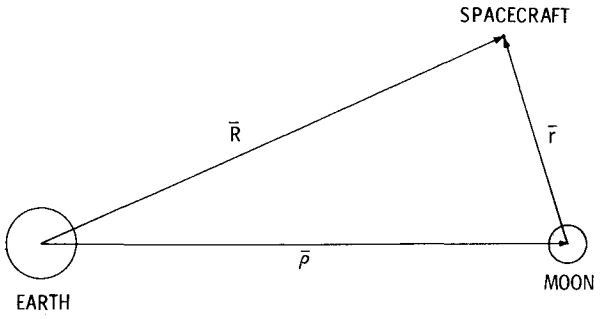

Fig. 1 Geometry of the restricted three-body problem.

$$\bar{R}_J = \bar{r}_J + \bar{\rho}_J \tag{4}$$

$$\dot{\bar{R}}_J = \dot{\bar{r}}_J + \dot{\bar{\rho}}_J \tag{5}$$

Given the state vector at some time t_I, the state vector at some later time t_F is desired.

A detailed derivation of Wilson's multiconic method is presented in Ref. 17. Wilson's multiconic approximation to the integration of the three-body differential equations of motion results in the following set of formulas for a trajectory moving away from the moon and towards the earth

$$\dot{\bar{R}}_{FAI} \cong \dot{\bar{r}}_{IaF} + \dot{\bar{\rho}}_I + \mu(\dot{\bar{\rho}}_F - \dot{\bar{\rho}}_I) \tag{6}$$

$$\bar{R}_{FAI} \cong \bar{r}_{IaF} + \bar{\rho}_I - (t_F - t_I)\dot{\bar{r}}_{IaF} + \mu[\bar{\rho}_F - \bar{\rho}_1 - (t_F - t_1)\dot{\bar{\rho}}_F] \tag{7}$$

where

$$\mu = a/(A+a) \cong 1/82.3 \tag{8}$$

The compound subscript denotes a vector resulting from the conic propagation of some initial state vector. For example, $\bar{\rho}_{IaF}$ is the position vector obtained by propagating the initial state vector $(t_I, \bar{\rho}_I, \dot{\bar{\rho}}_I)$ along a conic trajectory to t_F using α as the gravitational parameter. Since conic propagation is reversible, the position and velocity at the final time are obtained from

$$\dot{\bar{R}}_F = \dot{\bar{R}}_{(FAI)AF} \tag{9}$$

$$\bar{R}_F = \bar{R}_{(FAI)AF} \tag{10}$$

Simply stated, Eqs. (6) and (7) give formulas for the particular geocentric position and velocity which, if propagated forward in time by an amount $(t_F - t_I)$ along a geocentric conic, yield a position and velocity close to that which would result from propagating $R_I, \dot{R}_I$ forward in time to t_F along the actual three-body trajectory. If the spacecraft is moving towards the moon, and away from the Earth, a set of formulas for $\bar{r}_{FaI}$ and $\dot{\bar{r}}_{FaI}$ is obtained by Wilson. A simple way to obtain these formulas is to solve for $\bar{r}_{IaF}$ and $\dot{\bar{r}}_{IaF}$ in Eqs. (6) and (7) and interchange the subscripts I and F

$$\dot{\bar{r}}_{FaI} = \dot{\bar{R}}_{IAF} - \dot{\bar{\rho}}_F + \mu(\dot{\bar{\rho}}_F - \dot{\bar{\rho}}_I) \tag{11}$$

$$\bar{r}_{FaI} = \bar{R}_{IAF} - \bar{\rho}_F - (t_F - t_I)(\dot{\bar{R}}_{IAF} - \dot{\bar{\rho}}_F) + \mu[\bar{\rho}_F - \bar{\rho}_I - (t_F - t_I)\dot{\bar{\rho}}_F] \tag{12}$$

In this study it is assumed that the conic of the moon's orbit about the Earth is a circle; that is, the Earth and the moon both move in circular orbits about their barycenter.

If the time interval $t_F - t_I$ is restricted to a maximum of about 30 hr the derived equations are valid in the entire Earth-moon space. The trajectory problem is as follows: given the initial position and velocity at t_o what will be the position and velocity at some later time t_f? The total time interval is divided into segments (t_I, t_F) and either Eqs. (6) and (7) or Eqs. (11) and (12) are used depending on whether the trajectory lies between periselenium and perigee or vice versa. If the trajectory passes through perigee or periselenium, the propagation procedure must be switched from one mode to the other.

The actual procedure, illustrated for the case of motion away from the moon [Eqs. (6) and (7)] is as follows: 1) propagate a selenocentric conic forward in time by $(t_F - t_I)$; 2) propagate the position linearly backwards in time to t_I along the velocity vector; 3) transform the position and velocity to the geocentric frame; 4) modify the position and velocity to account for the indirect effect of the moon's motion (terms involving μ); and 5) propagate a geocentric conic forward in time by $(t_F - t_I)$.

Each step in the trajectory propagation is broken down into the above five steps, two of which require the solution of the two-body Kepler problem. The total propagation therefore requires the solution of $2n$ Kepler problems where n is the number of steps in the propagation. A one-step multiconic approximation to a trajectory from the L_2 libration point to the moon is shown in Fig. 2.

State Transition Matrix

A great advantage of the multiconic method is that in addition to the position and velocity, the state transition matrix may also be found at the final time with no additional integrations or differentiations. Since the positions and velocities in each step are solutions of Kepler's problem, from each Kepler problem solution the state transition matrix for that particular two-body conic is also obtained easily. Referring to the five-step procedure above, it can be shown that the operations defined by steps 3 and 4 do not affect the state transition matrix, so that to obtain the state transition matrix for the entire propagation sequence, the state transition matrices of steps 1, 2, and 5 need only be multiplied sequentially.

The three-body state transition matrix may be calculated from

$$\Phi_{3B}(t_F, t_I) = \Phi_{2B}{}^{(2)}(t_F, t_I)\Phi_L(t_I, t_F)\Phi_{2B}{}^{(1)}(t_F, t_I) \tag{13}$$

where the superscript (1) refers to the conic of the first step in the above five-step procedure and (2) refers to the second conic (step 5). The matrix $\Phi_L(t_F, t_I)$ is the state transition matrix of a linear (field-free) trajectory and is defined as

$$\Phi_L(t_F, t_I) = \begin{bmatrix} I & (t_F - t_I)I \\ 0 & I \end{bmatrix} \tag{14}$$

The product of the last two matrices on the right hand side of Eq. (13) causes the position derivatives of $\Phi_{2B}{}^{(1)}(t_F, t_I)$ to be backdated along the corresponding velocity derivatives by an amount $(t_F - t_I)$. Thus an analogous procedure may be stated for calculating the three-body state transition matrix for each step of the propagation: 1) from the first two-body conic obtain the two-body state transition matrix; 2) backdate the position derivatives along the corresponding velocity derivatives by an amount $(t_F - t_I)$; and 3) premultiply by the two-body state transition matrix of the second conic.

The state transition matrix for the whole trajectory is found by sequentially multiplying the state transition matrices for each step.

While a rigorous error analysis of the multiconic method has not been performed, it appears that step sizes of the order of 2–3 hr produce exceptionally accurate results, good to within

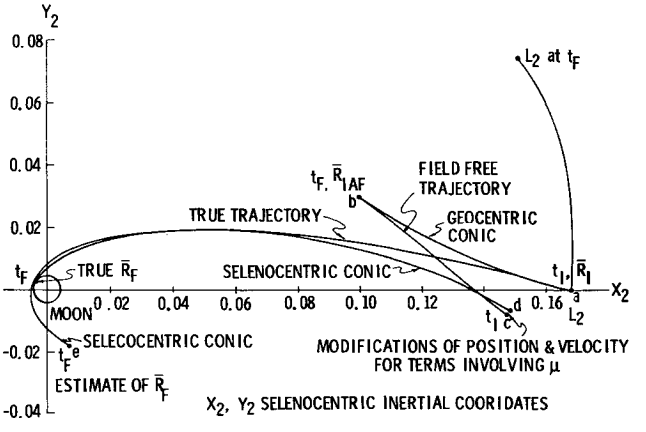

Fig. 2 True trajectory and 1 step multiconic approximation: L_2 to $\dot{R} = 0$ at moon in 48 hr.

about 0.1 fps in velocity and about 0.2 miles in position, while a step size of the order of 6 hr produces results accurate to within about 2–3 fps in velocity and 2–3 miles in position, certainly good enough for mission studies. Step sizes over 6 hr but less than 30 hr are useful, as it appears now, only for obtaining an intuitive feeling for the actual trajectory.

Two-Point Boundary Value Problems

The previous section dealt with the solution of the trajectory propagation problem for the restricted problem of three bodies by means of a multiconic method. That problem may be thought of as the three-body Kepler problem. This section considers the two-point boundary value problem of finding the initial velocity to satisfy given initial and final positions and a time of flight. This problem is the three-body Lambert problem. The multiconic method is ideally suited to solving this problem since as was noted in the previous section, the solution to the three-body Kepler problem furnishes in addition to the position and velocity at the final time, also the state transition matrix containing the partials of position and velocity at the final time with respect to the initial conditions. The three-body Lambert problem is solved by iterating on the unknown initial velocity to reduce the position error at the final time to zero. Since analytic partials are available, a Newton-Raphson (gradient) method is used.

Derivations of the solutions to two types of Lambert problems are given in Ref. 17. The two Lambert problems differ in the desired end conditions only. In one the desired end condition is a fixed final position vector. In the other the desired end condition is a given position magnitude and zero radial velocity. These two solutions were coded into a three-body Lambert routine.

Minimum Impulse Program

The previous two sections examined a multiconic method of trajectory propagation and the method used to solve the three-body Lambert problem. This section explains the application of primer vector theory to the determination of minimum-impulse (fuel-optimal) trajectories and describes the structure of the minimum impulse program which finds these trajectories.

The necessary conditions for optimality of an impulsive trajectory were formulated by Lawden[18] and are stated in terms of the primer vector which is the adjoint vector of the velocity vector in the optimal control problem. The four necessary conditions for optimality are: 1) the primer vector and its first derivative are everywhere continuous; 2) whenever an impulse occurs, the primer vector is aligned with the impulse and has unit magnitude; 3) the primer vector magnitude must not exceed unity on a coating arc; and 4) the time derivative of the primer vector magnitude must be zero at all interior junction points separating coasting arcs.

Figure 3(a) shows an optimal primer vector history for a two-impulse (Lambert) solution. Figures 3(b) and 3(c) show non-optimal two-impulse primer histories; Fig. 3(d) shows a non-optimal three-impulse primer vector history; and Fig. 3(e) shows an optimal three-impulse primer vector history. The primer vector, $\bar{\lambda}$, and its derivative propagate in the same manner as variations in position and velocity, i.e., by means of the state transition matrix

$$\begin{bmatrix}\bar{\lambda}(t)\\ \dot{\bar{\lambda}}(t)\end{bmatrix}=\begin{bmatrix}\phi_{11}(t,t_o) & \phi_{12}(t,t_o)\\ \phi_{21}(t,t_o) & \phi_{22}(t,t_o)\end{bmatrix}\begin{bmatrix}\bar{\lambda}(t_o)\\ \dot{\bar{\lambda}}(t_o)\end{bmatrix} \tag{15}$$

On any two-impulse trajectory (or any two-impulse segment of an n-impulse trajectory) the primer vector has the following boundary conditions

$$\bar{\lambda}(t_o)=\bar{\lambda}_o=(\Delta\bar{v}_o/|\Delta\bar{v}_o|) \qquad \bar{\lambda}(t_f)=\bar{\lambda}_f=(\Delta\bar{v}_f/|\Delta\bar{v}_f|) \tag{16}$$

where $\Delta\bar{v}_o$ and $\Delta\bar{v}_f$ are the impulses at the initial and final times, respectively. The initial value of the primer derivative may be found from one of the vector relations in Eq. (15) and is given by

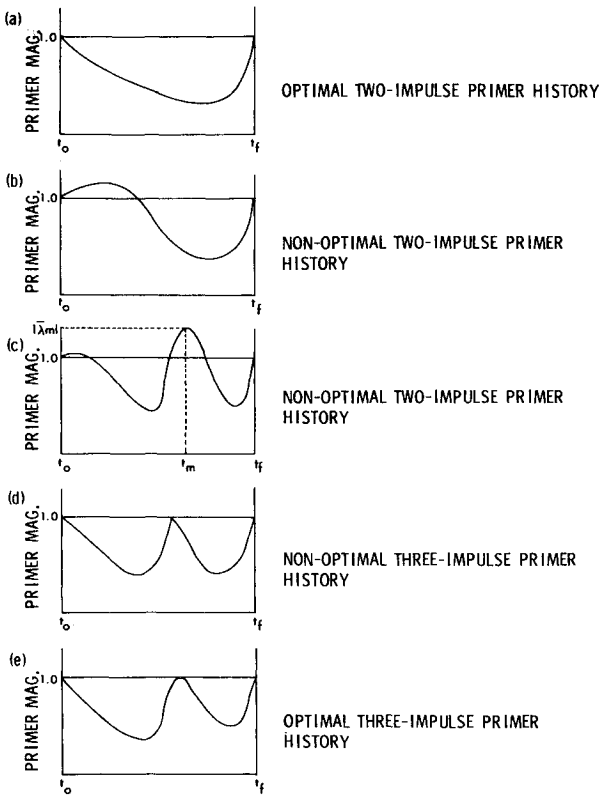

Fig. 3 Typical primer vector histories.

$$\dot{\bar{\lambda}}_o=\phi_{12}^{-1}(t_f,t_o)[\bar{\lambda}_f-\phi_{11}(t_f,t_o)\bar{\lambda}_o] \tag{17}$$

Knowing $\bar{\lambda}_o$, $\dot{\bar{\lambda}}_o$, and $\phi(t,t_o)$, a primer vector history can be generated.

The trajectory optimization method developed for the two-body problem in Ref. 3 may be carried over directly to the three-body problem. A full derivation of the method is contained in Ref. 3. The remainder of this section is an outline of the procedure for finding fuel optimal impulsive trajectories (this outline also gives the structure of the minimum impulse program).

1) Given the initial and final state vectors (position and velocity) and the transfer time, solve the three-body Lambert problem to find the two-impulse reference solution. [The state transition matrix, $\phi(t_f,t_o)$, is also obtained.]

2) Compute $\bar{\lambda}_o$, $\bar{\lambda}_f$, and $\dot{\bar{\lambda}}_o$ according to

$$\bar{\lambda}_o=\Delta v_o/|\Delta\bar{v}_o|, \qquad \bar{\lambda}_f=\Delta\bar{v}_f/|\Delta\bar{v}_f|$$
$$\dot{\bar{\lambda}}_o(t)=\phi_{12}^{-1}(t_f,t_o)[\bar{\lambda}_f-\phi_{11}(t_f,t_o)\bar{\lambda}_o]$$

and generate the primer vector history (this involves calling the trajectory propagation program once) according to

$$\bar{\lambda}(t)=\phi_{11}(t,t_o)\bar{\lambda}_o+\phi_{12}(t,t_o)\dot{\bar{\lambda}}_o$$

[$\lambda(t)$ can be computed at as many points as there are steps in the trajectory propagation.]

3) Examine the primer history and if $|\bar{\lambda}(t)|$ exceeds unity anywhere between the initial and final times the two-impulse trajectory is not optimal and a third impulse is added at t_m, the time at which $|\bar{\lambda}(t)|$ is maximum

$$\delta\bar{r}_m=cA^{-1}\bar{\lambda}_m/|\bar{\lambda}_m|$$
$$A=\phi_{22}(t_m,t_f)\phi_{12}^{-1}(t_m,t_f)-\phi_{22}(t_m,t_o)\phi_{12}^{-1}(t_m,t_o)$$

[From the examination of the primer history, t_m and $\bar{\lambda}_m$ are found directly; the trajectory routine must be called once more to compute $\phi(t_m,t_o)$; from $\phi(t_f,t_o)$ and $\phi(t_m,t_o)$, all the matrices needed for the calculation of the A matrix may be found. The quantity c is the magnitude of the additional impulse and should be small.]

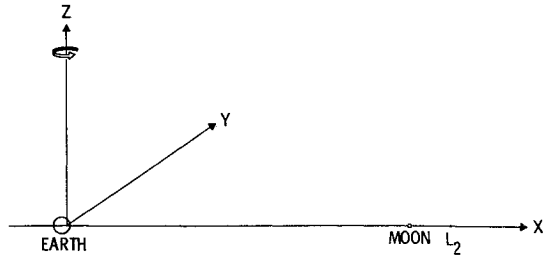

Fig. 4 Rotating barycentric coordinate system.

4) Solve two three-body Lambert problems: a) from the initial position to $\bar{r}_m+\delta\bar{r}_m$ with transfer time t_m-t_o, and b) from $\bar{r}_m+\delta\bar{r}_m$ to the given final position with transfer time t_f-t_m. This yields a nonoptimal three-impulse trajectory. Use the Jacobson-Oksman minimization algorithm[16] to iterate on $\bar{r}_m$ and t_m to minimize the total cost. The cost for each new $\bar{r}_m$ and t_m is found by again solving two three-body Lambert problems. The gradient is calculated from

$$\partial J/\partial\bar{r}_m = (\dot{\bar{\lambda}}_m^{\,+} - \dot{\bar{\lambda}}_m^{\,-})^T$$
$$\partial J/\partial t_m = -(\dot{\bar{\lambda}}_m^{\,+T}\bar{v}_m^{\,+} - \dot{\bar{\lambda}}_m^{\,-T}\bar{v}_m^{\,-})$$

where + and − refer to just after and before the third impulse, respectively. All these quantities can be found from the output of the three-body Lambert solutions.

5) Check the primer history of the converged trajectory—if the necessary conditions are satisfied, the program is finished; if not, another impulse is added and the convergence process is started again.

It should be noted that the preceding theory and procedure will calculate minimum impulse trajectories only between fixed initial and final states. The position at the final time is fixed throughout the convergence procedure. Variable end constraints are not permissible at this time but certain constraints can be handled in other ways. For instance, the optimal transfer to a circular orbit can be found by successively solving problems to a fixed final position of the desired magnitude such that the final position is varied on a circle. Of course the proper velocity at each position to establish a circular orbit at that altitude must be supplied (or calculated within the program).

Another version of the program was also written which accepts a starting three-impulse solution and begins convergence to the optimal trajectory immediately. Also, some existing three-impulse solutions, the optimality of which is of interest, do not readily derive from two-impulse solutions.

Results

The basic coordinate system used is a rotating barycentric coordinate system. The x-axis points along the Earth-moon line towards the moon, the z-axis is perpendicular to the Earth-moon plane, and the y-axis is in the plane so as to form a right-handed system. This system and the L_2 libration point are shown in Fig. 4.

Fast Two-Impulse Trajectories between the Moon and L_2

The units used in the programs are such that the unit of mass is the sum of the masses of the Earth and the moon, the unit of distance is the Earth-moon distance, and the unit of time is chosen so that the angular velocity of the Earth-moon line is equal to 1. Conversion factors are given below: 1 unit of distance = 384410 km, 1 unit of time = 104.362 hr, 1 unit of velocity = 1023.17 m/sec.

All trajectories in this study start at the L_2 libration point and end at either the moon or the Earth; all trajectories are in the Earth-moon plane. Trajectories from a body to L_2 are found by reflecting the trajectories in this study about the y-axis.

Utilizing the three-body Lambert routine, a family of relatively fast trajectories between the L_2 libration point and a 185.2 km circular orbit about the moon was found. The routine was run

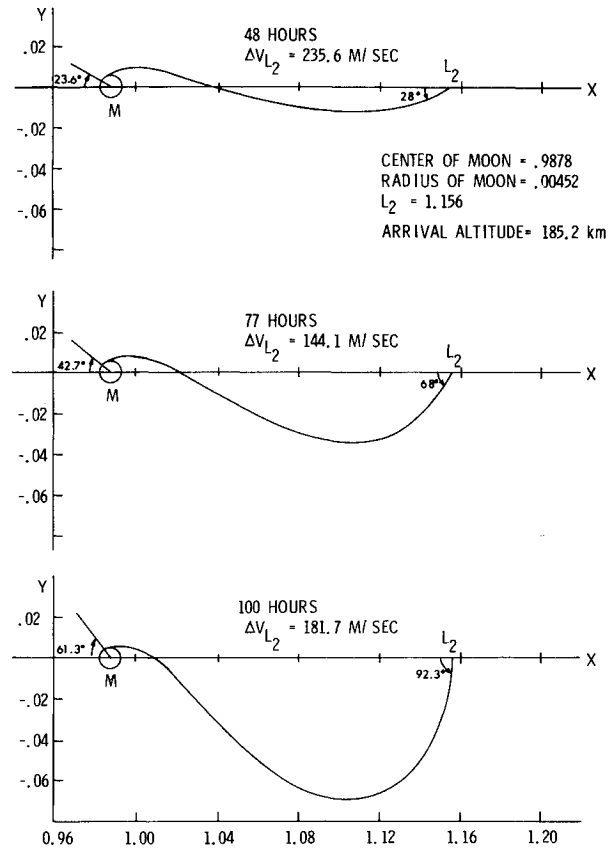

Fig. 5 Fast two-impulse trajectories between the moon and L_2.

in the mode which converges to a desired radius magnitude with no radial velocity. Thus a tangential impulse at the moon will establish the spacecraft in a circular orbit. Trajectories were found with transfer times from 48 to 100 hr. Three of these trajectories are shown in Fig. 5, and the transfer times, the

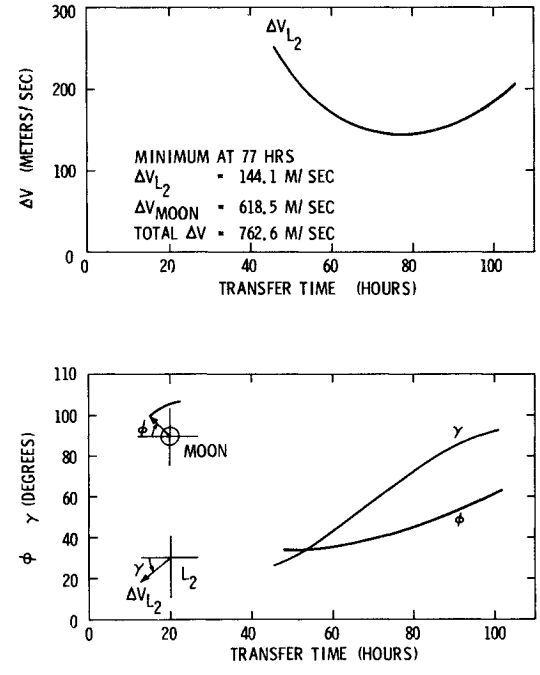

Fig. 6 ΔVs and departure and arrival angles for fast two-impulse trajectories between the moon and L_2.

magnitudes of the impulses at L_2, and the departure and arrival angles are indicated for each.

In Fig. 6, the magnitude of the impulse at L_2 and the departure and arrival angles are plotted vs transfer time. The minimum two-impulse transfer for this family occurs at about 77 hr. The impulse at L_2 is 144.1 m/sec, the impulse at the moon is 618.5 m/sec, and the total cost is thus 762.6 m/sec.

The three trajectories in Fig. 5 correspond to transfer times less than, equal to, and greater than the transfer time for the minimum impulse transfer. By computing the primer vector histories for these trajectories we can determine if an additional impulse will decrease the total cost. If the magnitude of the primer vector rises above unity anywhere between the initial and final times, adding an impulse will decrease the total cost. The primer histories for the three trajectories in Fig. 5 are given in Fig. 7.

Note, first of all, that the derivative of the primer magnitude at the initial time is zero for the minimum impulse 77-hr transfer. Although it cannot be seen on the plot, the derivative is zero at the final time also. This situation is true of all minimums with respect to time of flight. The primer history indicates that either increasing or decreasing the transfer time by slightly changing the initial or final times will not affect the cost since the primer magnitude approaches unity asymptotically at both the initial and final times. Since the cost is a minimum at 77 hr, the gradient of the cost with respect to transfer time is indeed zero at this transfer time.

Secondly, it can be seen that trajectories with transfer times less than or equal to that of the minimum are locally optimal while trajectories with transfer times greater than that of the minimum are not. These nonoptimal trajectories can be improved by an additional impulse in the direction of the primer vector at its maximum. However, because the primer vector history for the transfer time which yields the minimum cost does not rise above unity, there exists no three-impulse solution which requires less cost in the neighborhood of this two-impulse solution. The minimum two-impulse solution is locally optimal. It has been shown[2] that for primer vector histories of the type which occurred for the 100-hr transfer, the cost can be improved by an initial coast. If a third impulse were added for the 100-hr transfer at the maximum of the primer magnitude and an iteration started to converge to an optimal three-impulse solution, what would occur is that the interior impulse would grow in magnitude and the initial impulse would decrease and eventually disappear. The optimal solution for 100 hr is to coast for 23 hr (remain at L_2) and then apply an impulse to transfer to the moon in 77 hr. For any time of flight greater than that of the minimum two-impulse solution, the optimal trajectory is an initial coast until the time remaining is equal to the transfer time of the minimum two-impulse trajectory and then a minimum two-impulse transfer.

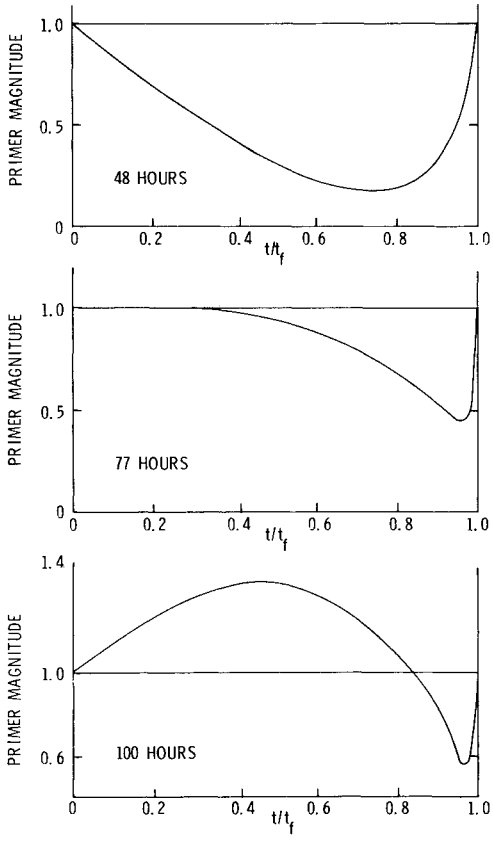

Fig. 7 Primer histories for fast two-impulse trajectories between the moon and L_2.

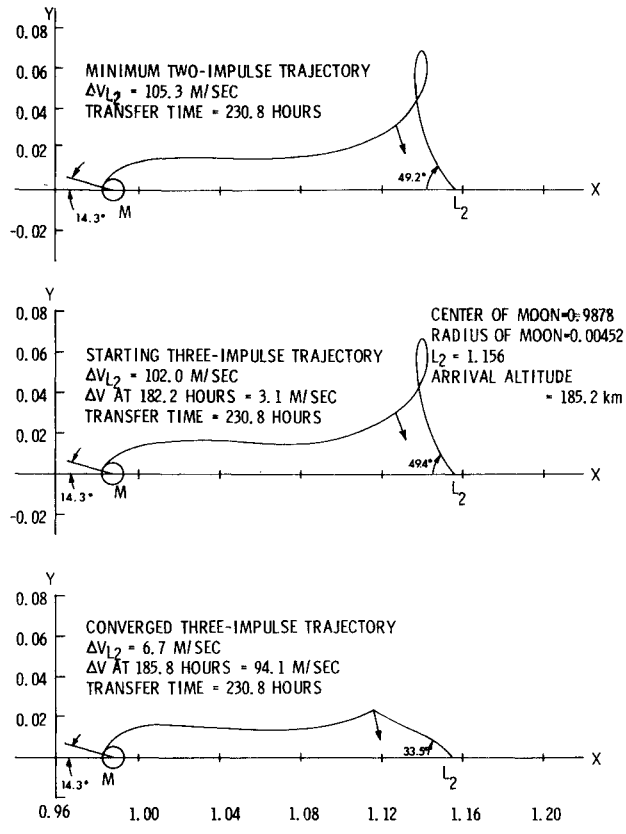

Fig. 8 Slow two-impulse trajectories between the moon and L_2.

A family of slower two-impulse trajectories between the moon and L_2 which have smaller ΔV requirements will be investigated in the next section. There does exist[10] another family of trajectories which arrive at the trailing side of the moon (negative ϕ) but these trajectories have even higher ΔV requirements than the fast trajectories of this section and for that reason, they were not investigated.

Slow Two-Impulse Trajectories between the Moon and L_2

Another family of two-impulse transfers between the moon and L_2 was found with transfer times ranging between 209–254.4 hr. These transfers are quite slow compared to the family discussed in the previous section. Three of the trajectories are plotted on Fig. 8: one for a transfer time below the minimum, one for the transfer which yields the minimum cost, and one

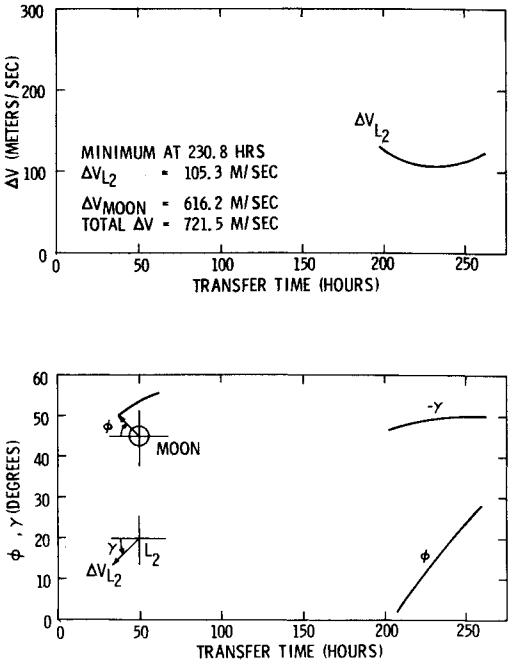

Fig. 9 ΔVs and departure and arrival angles for slow two-impulse trajectories between the moon and L_2.

for a transfer time greater than the minimum. The ΔV requirement at L_2 as a function of transfer time and the departure and arrival angles are given on Fig. 9. The minimum two-impulse trajectory for this family has a transfer time of about 230.8 hr.

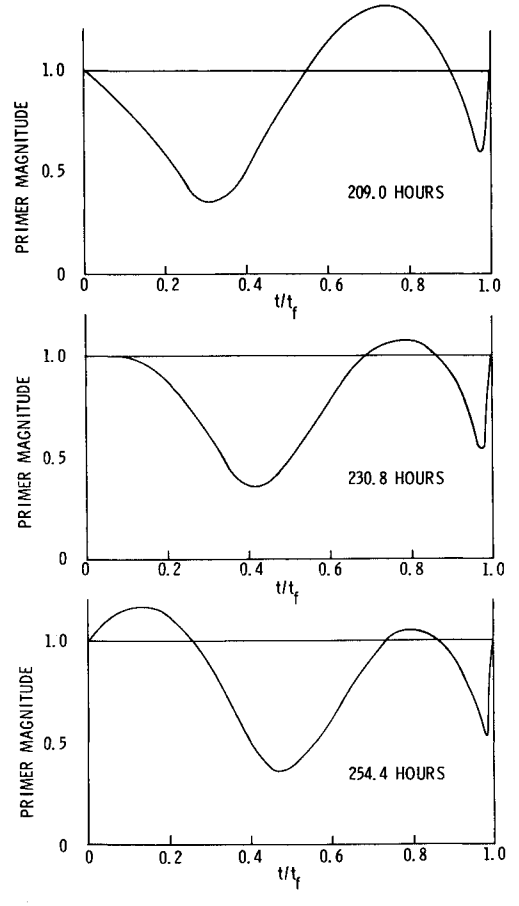

Fig. 10 Primer histories for slow two-impulse trajectories between the moon and L_2.

The required impulse at L_2 is 105.3 m/sec; the impulse at the moon is 616.2 m/sec; the total cost is thus 721.5 m/sec. These values compare to 114.1 m/sec, 618.5 m/sec, and 762.6 m/sec for the minimum two-impulse solution for the fast family of the previous section. The minimum two-impulse solution for the slow family is 5.4% cheaper in total cost than that for the fast family. The impulse at L_2 is 26.9% smaller. It appears that all the trajectories in this family have a distinctive cusp or loop when plotted in the rotating barycentric coordinate system.

The primer vector histories for the three trajectories shown in Fig. 8 are given in Fig. 10. When compared to the primer vector histories of the fast family (Fig. 7), certain similarities appear. Note once again that the primer history for the minimum cost transfer necessarily has a zero derivative at the initial time (and also, although unapparent, at the final time) since it is a minimum with respect to time of flight. All trajectories with times of flight greater than that of the minimum can be improved by an initial coast since the primer magnitude rises above unity immediately after the initial impulse.

However it can clearly be seen that none of the primer vector histories satisfy the necessary conditions for a local optimum. From the behavior of the three primer histories on Fig. 10, it is evident that all primer histories for trajectories with transfer times less than that of the minimum have one maximum above unity. Also, all trajectories with transfer times greater than that of the minimum will have two maximums. The first is always above unity and the second will be above unity up to some transfer time, as yet undetermined, but greater than 254.4 hr at which the second maximum will be exactly equal to 1. Beyond this undetermined transfer time, the second maximum will be below unity. The arrows on Fig. 8 show the location, direction, and magnitude of the primer vector at the second maximum. The third impulse would be added in this direction.

Most importantly, it should be noted that the primer history for the minimum impulse solution does not satisfy the necessary

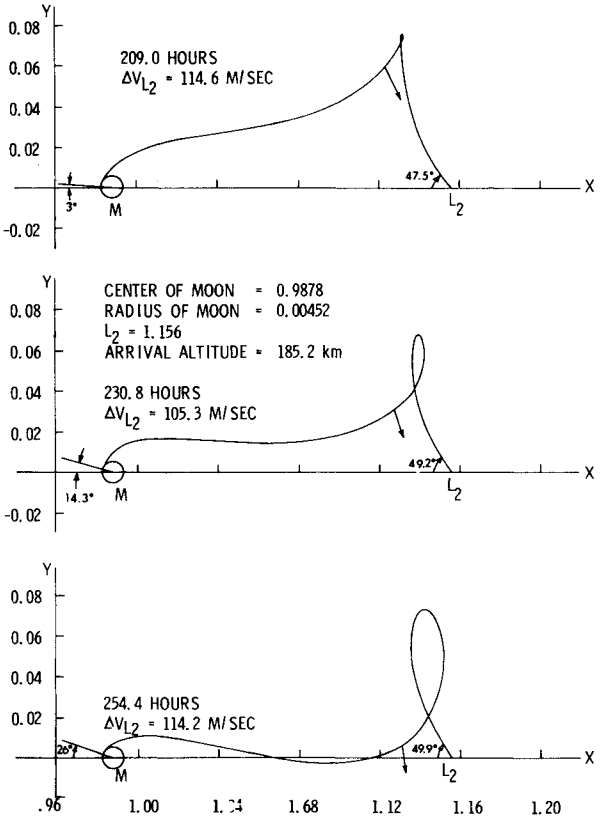

Fig. 11 Two- and three-impulse trajectories between the moon and L_2.

conditions for a local optimum because the second maximum is still above unity. Thus there does exist a neighboring three-impulse solution which requires less cost than the minimum two-impulse solution for this slow family. Recall that on the contrary, the minimum two-impulse solution for the fast family was locally optimal. It is believed that the three-impulse solutions which can be derived from the nonoptimal minimum two-impulse solution at 230.8 hr have never before been investigated. Some of these trajectories are discussed in the following section.

Three-Impulse Trajectories between the Moon and L_2

The minimum impulse program was used to add a third impulse to the nonoptimal minimum two-impulse solution of the previous section and converge to a minimum three-impulse solution. Pictured in Fig. 11 are three trajectories. The top one is the nonoptimal minimum two-impulse solution. The middle trajectory is the starting three-impulse solution which results from adding a small impulse of chosen magnitude in the direction of the primer vector at its maximum on the non-optimal minimum two-impulse solution. The bottom trajectory is the solution to which the minimum impulse program converged. Note that the loop has disappeared in the converged three-impulse trajectory.

The arrows in the figure give the location, direction, and magnitude of the primer vector at the interior impulse. For the nonoptimal minimum two-impulse trajectory the arrow points in the direction that an impulse would be added. Hence the direction and location are the same for the upper two trajectories. The magnitude of the primer vector at the interior impulse is necessarily equal to 1 for the lower two trajectories. The minimum two-impulse trajectory differs very little from the starting three-impulse trajectory since the magnitude of the interior impulse is small.

The minimum two-impulse trajectory has a 105.3 m/sec impulse at L_2 and a 616.2 m/sec impulse at the moon for a total cost of 721.5 m/sec (see Fig. 8). The converged three-impulse trajectory has a 6.7 m/sec impulse at L_2, a 94.1 m/sec impulse 185.8 hr after leaving L_2, and a 612.9 m/sec impulse at the moon, for a total cost of 713.7 m/sec. The total cost is 1.1% cheaper whereas excluding the impulse at the Earth, the improvement is 4.3%. Comparing the starting three-impulse trajectory to the converged three-impulse trajectory, it can be seen that the interior impulse has grown to almost the magnitude of the original impulse at L_2. Consequently the impulse at L_2 has become quite small.

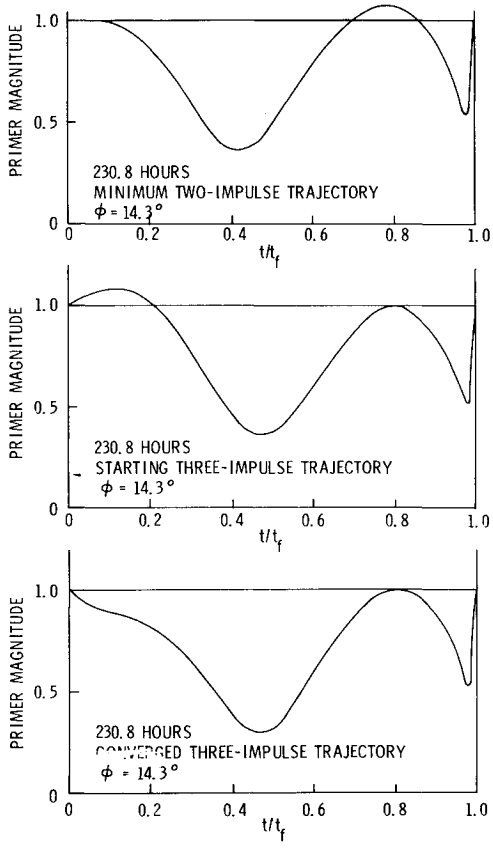

Fig. 12 Primer histories for two- and three-impulse trajectories between the moon and L_2.

The primer histories associated with the three trajectories in Fig. 11 are given in Fig. 12. Note that the primer histories for the minimum two-impulse solution and the starting three-impulse solution do not satisfy the necessary conditions. However, the primer history for the converged three-impulse solution does. For two-impulse histories the necessary conditions are also sufficient for a local two-impulse optimum.[19] The conclusions for the fast two-impulse trajectories use this fact. For three-impulse histories the necessary conditions are not sufficient for a local three-impulse optimum. However, satisfaction of these necessary conditions in conjunction with an accelerated gradient search procedure does yield a sufficiency condition for three impulses except under unusual circumstances. The Jacobson algorithm iterates to reduce the cost function at each step such that a minimum is eventually found. If a neighboring three-impulse solution existed which also satisfied the primer necessary conditions but was not a minimum (such as a saddle-point), the algorithm would almost certainly not converge to it, because an accelerated gradient search procedure reduces the cost at each step and cannot normally converge to anything but a local minimum. Thus it can be stated that since the primer magnitude for the converged three-impulse solution does not exceed unity, there exists no neighboring four-impulse solution with less cost.

Recall that the minimum impulse program finds the trajectory with minimum total cost with respect to the time and position of the interior impulse by iterating to force the derivative of the primer magnitude to be continuous and equal to zero at the interior impulse. The theory requires that the initial and final states and the transfer time be fixed during the iteration. Hence the arrival angle, ϕ, may be varied keeping the altitude fixed at 185.2 km and a minimum found over a set of converged three-impulse solutions. This was done and it was found that the original converged three-impulse solution ($\phi = 14.3°$) was the minimum of total cost with respect to arrival angle. The derivative of the primer magnitude at the initial time for this converged three-impulse trajectory is negative as can be seen in Fig. 12. For a minimum with respect to transfer time, it is zero (see Figs. 7 and 10). This indicates that lengthening the transfer time will improve the total cost. Ideally for various transfer times, the minimum with respect to arrival angle should be found and then the minimum of this set of solutions would give the minimum three-impulse transfer between L_2 and a 185.2 km circular orbit about the moon. Another method would be to reformulate the iteration to include variable end conditions.

Since the final position is fixed during iteration, the final impulse is not necessarily tangential as it was for the minimum two-impulse solution. Thus the final state may be preperiselenium or postperiselenium. The converged three-impulse trajectory for an arrival angle of 14.3° nevertheless arrives almost exactly at periselenium.

Conclusions

1) A multiconic approach can be used for rapid and efficient calculations of optimal multiple impulse trajectories in the three-body problem.

2) There exist locally optimal families of two-impulse transfers between the L_2 libration point and the moon. These families generally involve the shortest flight times.

3) The "slow" family of two-impulse transfers between L_2 and the moon previously found by Nicholson of GE[9] is not locally optimal. However, three-impulse transfers generated from this family are locally optimal. These require more time but less fuel than the fast transfers.

References

[1] Gobetz, F. W. and Doll, J. R., "A Survey of Impulsive Trajectories," *AIAA Journal*, Vol. 7, No. 5, May 1969, pp. 801–834.

[2] Lion, P. M. and Handelsman, M., "Primer Vector on Fixed Time Impulsive Trajectories," *AIAA Journal*, Vol. 6, No. 1, Jan. 1968, pp. 127–132.

[3] Jezewski, D. J. and Rozendaal, H. L., "An Efficient Method for Calculating Optimal Free-Space *N*-Impulse Trajectories," *AIAA Journal*, Vol. 6, No. 11, Nov. 1968, pp. 2160–2169.

[4] Gobetz, F. W. and Doll, J. R., "How to Open the Heliocentric Launch Window for Earth-Mars Orbiter Missions," *Journal of Spacecraft and Rockets*, Vol. 6, No. 4, April 1969, pp. 353–359.

[5] Egorov, V. A., "Certain Problems of Moon Flight Dynamics," *Russian Literature on Satellites*, Part I, International Physical Index, Inc., New York, 1958.

[6] Breakwell, J. V. and Perko, L. M., "Matched Asymptotic Expansions, Patched Conics, and the Computation of Interplanetary Trajectories," *AIAA Progress in Astronautics and Aeronautics: Methods in Astrodynamics and Celestial Mechanics*, Vol. 17, edited by R. L. Duncombe and V. G. Szebehely, Academic Press, New York, 1966, pp. 159–182.

[7] Lagerstorm, P. A. and Kevorkian, J., "Earth-to-Moon Trajectories in the Restricted Three-Body Problem," *Journal Mécanique*, Vol. 2, No. 2, June 1963.

[8] Lancaster, J. E. and Allemann, R. A., "Numerical Analysis of the Asymptotic Two-Point Boundary Value Solution for *N*-Body Trajectories," *AIAA Journal*, Vol. 11, No. 3, March 1973, pp. 259–260.

[9] "Final Report for Lunar Libration Point Flight Dynamics Study," NASA Contract NAS-5-11551, April 1969, The General Electric Co., Philadelphia, Pa.

[10] Edelbaum, T. N., "Libration Point Rendezvous," Rept. 70-12, Feb. 1970, Analytical Mechanics Associates, Cambridge, Mass.

[11] Farquhar, R. W., "The Utilization of Halo Orbits in Advanced Lunar Operations," TND-6365, July 1971, NASA.

[12] Stumpff, K. and Weiss, E. H., "Applications of an *N*-Body Reference Orbit," *Journal of the Astronautical Sciences*, Vol. 15, No. 5, Sept.–Oct. 1968.

[13] Wilson, S. W., "A Pseudostate Theory for the Approximation of Three-Body Trajectories," AIAA Paper 70-1061, Santa Barbara, Calif., 1970.

[14] Byrnes, D. V. and Hooper, H. L., "Multiconic: A Fast and Accurate Method of Computing Space Flight Trajectories," AIAA Paper 70-1062, Santa Barbara, Calif., 1970.

[15] Weiss, E. H., "A New Method for Computing the State Transition Matrix," *Journal of the Astronautical Sciences*, Vol. 16, No. 3, May–June 1969.

[16] Jacobson, D. and Oksman, W., "An Algorithm that Minimizes Homogeneous Functions of N Variables in $N+2$ Iterations and Rapidly Minimizes General Functions," TR 618, Oct. 1970, Harvard Univ., Div. of Engineering and Applied Physics, Cambridge, Mass.

[17] D'Amario, L. and Edelbaum, T. N., "Minimum Impulse Three-Body Trajectories," AIAA Paper 73-145, Washington, D.C., 1973.

[18] Lawden, D. F., *Optimal Trajectories for Space Navigation*, Butterworths, London, 1963.

[19] Lion, P. M., "Sufficient Conditions for Optimal Fixed-Time Impulsive Trajectories," presented at the 18th International Congress, Belgrade, Sept. 1967.